

# Stagnation Line and Upwash Formation of Two Impinging Jets

M. J. Siclari,\* W. G. Hill Jr.,\* and R. C. Jenkins†  
*Grumman Aerospace Corporation, Bethpage, N. Y.*

When two jets in reasonable proximity exhaust into ambient surroundings and impinge on a ground plane, radial wall jets are formed which interact and form a stagnation region. The flow then is deflected upward to form an "upwash" sheet. These individual upwash flows are the heart of the complicated effects experienced by VTOL aircraft when they operate in ground proximity. It is the intent of this study to develop relatively simple flow models and prediction techniques, based primarily on momentum principles and empirical observations, for the estimation of two-jet ground impingement phenomena. Comparisons with experimental data indicate that these simple computational techniques can yield very reasonable estimates of certain overall aspects of the two-jet impingement problem.

## Nomenclature

$a_w$	= slope of wall jet thickness growth
$b_v$	= local velocity profile length scale
$C_s$	= similarity constant
$d$	= jet diameter
$i_r$	= radial unit vector
$i_u$	= upwash unit vector
$i_x, i_y, i_z$	= ground fixed Cartesian unit vectors
$I$	= momentum density
$M$	= radial momentum
$r, \phi$	= local ground plane polar coordinate system
$V$	= velocity
$x, y, z$	= ground fixed Cartesian coordinate system
$\rho$	= density
$\sigma$	= jet inclination angle, 90 deg defined as vertical
$\theta$	= local stagnation line slope

## Subscripts

$F$	= flux
$g$	= ground plane
$J$	= jet or wall jet
$m$	= maximum value in profile
$n$	= upwash flow element
$N$	= normal component
$s$	= stagnation line
$u$	= upwash flow

## Introduction

THE extreme complexity of VTOL flowfields does not allow for a rigorous treatment short of solving the complete three-dimensional Navier-Stokes equations. In recent years, however, a need has been established for less rigorous approaches to this problem that nevertheless can provide important information about the behavior of such flowfields.<sup>1-5</sup> This study reports on one such approach to a subset of the overall VTOL problem, namely, two-jet ground impingement and resultant wall jet interaction. The two-jet impingement problem that results in an upwash flow is considered to be a very basic and essential problem. These upwash flows are believed to be the heart of the complicated fountain effects experienced by VTOL aircraft when they operate in-ground effect. "Central fountains" are formed in a multijet configuration due to the mutual coalescence of the individual upwash flows generated by any two impinging jets.

Hence, a basic understanding of the upwash flow would greatly enhance an eventual understanding of central fountain flows.

The approach of this study is to employ a "building block" or "modular flowfield concept" to the overall flowfield. The various components are defined to be the free jet, jet deflection, wall jet, upwash deflection, and free upwash zones. A mathematical model is then constructed for each zone based on empirical observations and global momentum constraints. During the course of the study, a series of experiments was conducted to validate and improve these flow models for the prediction of wall jet interaction phenomena generated by both oblique and unequal strength circular jets.

## Basic Two-Jet Impingement Interaction Characteristics

In general, when two circular jets impinge on a ground plane, radial wall jets are formed. Their collision and interaction forms a "stagnation line" and "upwash" region. If the two jets impinge vertically with equal momentum the stagnation line will be a straight line everywhere equidistant from the two-jet impingement centers. If the two jets have unequal momentum (e.g., unequal diameters or exit pressure) or are inclined at an angle other than 90 deg relative to the ground plane, the stagnation line will, in general, exhibit curvature (Fig. 1).

The flow is characterized by several distinct regions. The free jet region, where the jet decays as if the ground plane were not present, and the impingement region of the jet, where the flow decelerates to the ground stagnation point. The stagnation point is not, in general, coincident with the geometric jet impingement point. The flow then accelerates from the stagnation point until static pressure recovery has occurred throughout the wall layer and a radial wall jet has developed. Opposing wall jets collide and form a stagnation or upwash deflection region resulting in the upward deflection of the wall jet fluid. It has been shown experimentally that for a pair of two-dimensional colliding wall jets, the location of the stagnation region corresponds roughly to the position of equal maximum total pressure in the individual wall jet layers.<sup>6</sup> At some small distance above the ground plane, the two wall jets have fully merged and accelerated to form, in general, an asymmetric upwash free shear profile without any detectable residual evidence of the wall defect layer. The upwash flow will continue along a straight path, defined by the upwash inclination angle until some external influence, such as proximity to a free jet, disturbs this path. At each point in the upwash sheet, along the path of the stagnation line, the upwash generally exhibits large three-dimensional flow angularity. Far from the impingement centers of the jets, the upwash inclination tends to become tangential to the ground plane (i.e., excluding wall jet separation phenomena). If the upwash flow comes close to the free jet, a recirculation

Presented as Paper 77-615 at the AIAA/NASA Ames V/STOL Conference, Palo Alto, Calif., June 6-8, 1977; submitted May 12, 1980; revision received April 6, 1981. Copyright © 1981 by M. J. Siclari. Published by the American Institute of Aeronautics and Astronautics Inc., with permission.

\*Staff Scientist, Research Department.

†Research Scientist, Research Department. Member AIAA.

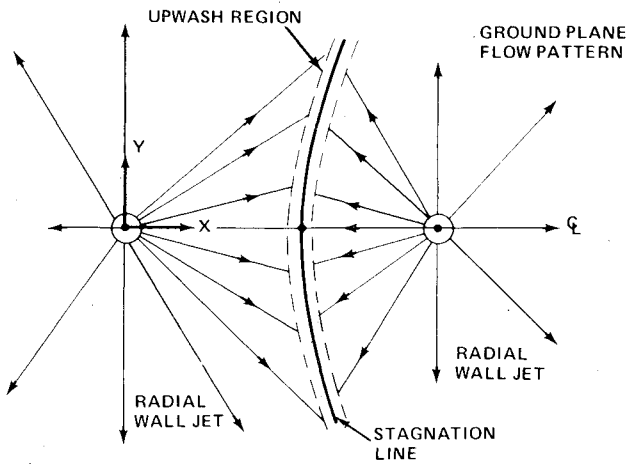


Fig. 1 Two-jet impingement interaction problem.

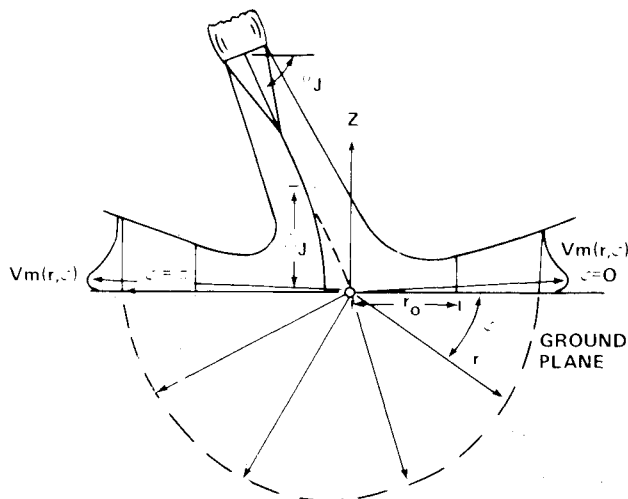


Fig. 2 Oblique jet impingement flow model.

of the upwash flow can occur, and has been visualized experimentally by several investigators.<sup>7,8</sup>

In the following sections, a simple and approximate mathematical model of the wall jet will be developed which will provide estimates of the stagnation line and three-dimensional upwash flow angularity.

### Generalized Wall Jet Momentum Model

The ultimate success of an analysis for the determination of stagnation lines and upwash inclination angles lies in a formulation of a wall jet momentum model which satisfies, at least to a first order, physically observable wall jet phenomena. The framework for the momentum modeling of wall jets, for the prediction of stagnation lines, was initially defined in Refs. 1 and 2 and shown to be successful for vertical jet impingement. Oblique jet impingement presents additional difficulties in modeling because of azimuthal asymmetry. The empirical data base for the modeling of isolated wall jets comes essentially from Refs. 9-11. Figure 2 shows the coordinate system and nomenclature adopted for the isolated wall jet problem.

Donaldson and Snedeker<sup>10,11</sup> made a number of significant observations with respect to free jet oblique impingement data. They showed that the momentum flux per unit radian of the wall jet was relatively invariant for different radii and that the assumption of flow sector independence was physically reasonable, which also implies that nonradial components of velocity could be assumed to be negligible.<sup>10</sup> Donaldson and Snedeker also observed that the wall jet thickness was relatively invariant with respect to azimuthal location, while

the maximum velocity of the wall layer exhibited a significant azimuthal variation. Thus, in the simplified analysis to follow, the wall jet thickness slope is assumed invariant with jet inclination angle and measured wall jet entrainment or the mass flow rate for vertical jet impingement is assumed applicable to individual flow sectors.

These empirical observations lead to the simplifying assumptions of radial velocity and linear growth of the wall layer along with flow similarity. The decay of the maximum wall jet velocity is taken to be hyperbolic with the characteristic functional form

$$V_m(r, \varphi) = \beta \Omega(K) f(K, \varphi) / r \quad (1)$$

where  $\beta = V_j d_j$  is a jet strength parameter and  $\Omega$  is a jet impingement factor which depends on  $K = K(\sigma_j)$ , a jet impingement angle parameter.

The magnitude of the radial momentum flux per unit radian of the wall jet can be expressed as

$$\frac{\partial M(\varphi)}{\partial \varphi} = \rho \int_0^\infty V^2(r, \varphi, Z) r dZ \quad (2)$$

which becomes, in vector notation

$$\frac{\partial M(\varphi)}{\partial \varphi} = \rho C_s r b_w V_m^2(r, \varphi) i_r \quad (3)$$

where  $C_s$  is a velocity squared similarity constant and  $a_w$  is the growth constant of the wall layer.

Upon substitution of Eq. (1)

$$\frac{\partial M(\varphi)}{\partial \varphi} = \rho C_s a_w \beta^2 \Omega^2 f^2(K, \varphi) i_r \quad (4)$$

The momentum flux defined by Eq. (4) is now a constant for any given (and assumed radial) streamline defined by  $\varphi = \text{const}$ , hence neglecting any momentum losses due to shear at the wall.

If an azimuthal form for the velocity distribution can be determined, the form of the azimuthal momentum flux distribution is then immediately known from Eq. (4).

The Kappa function of jet inclination angle can be determined by imposing the requirement that the x momentum of the radial wall jet is related to the total magnitude of the radial wall jet outflow momentum by the jet inclination and angle  $\sigma_j$ , or, simply,

$$\dot{M}_x = \dot{M} \cos \sigma_j \quad (5)$$

The x momentum of the radial wall jet can be expressed simply as

$$\dot{M}_x = \int_0^{2\pi} \left[ \frac{\partial M(\varphi)}{\partial \varphi} \cdot i_x \right] d\varphi = \int_0^{2\pi} \frac{\partial M(\varphi)}{\partial \varphi} \cos \varphi d\varphi \quad (6)$$

The total magnitude of the outflow or radial momentum of the wall jet is

$$\dot{M} = \int_0^{2\pi} \left[ \frac{\partial M(\varphi)}{\partial \varphi} \cdot i_r \right] d\varphi = \int_0^{2\pi} \frac{\partial M(\varphi)}{\partial \varphi} d\varphi \quad (7)$$

Substitution of Eq. (4) into Eqs. (6) and (7), and Eq. (5) leads to the following integral constraint required of the Kappa function

$$\int_0^{2\pi} f^2(K, \varphi) \cos \varphi d\varphi = \cos \sigma_j \int_0^{2\pi} f^2(K, \varphi) d\varphi \quad (8)$$

The above requirement supplies an expression for the Kappa function without regard to the actual magnitude of the total wall jet momentum. Now, if, in addition, a further requirement is imposed that the magnitude of the total radial outflow momentum of the wall jet is independent of the jet impingement angle, another integral constraint can be derived for the impingement factor  $\Omega(K)$ , viz

$$\Omega(K) = \left[ 2\pi / \int_0^{2\pi} f^2(K, \varphi) d\varphi \right]^{1/2} \quad (9)$$

Table 1 Inclined jet impingement parameters  
Cosine form:  $f(K, \varphi) = 1 + K \cos \varphi$

$\sigma_J$ , deg	$K$	$\Omega$
90	0.0	1.0
75	0.2681	0.9825
60	0.586	0.924
45	1.4142	0.7071

$$f(K, \varphi) = 1 + K(\sigma_J) \cos \varphi \quad (10)$$

This form of the azimuthal function satisfies symmetry requirements and implicitly requires that, in the limit, as  $\sigma_J \rightarrow \pi/2$ ,  $K(\sigma_J) \rightarrow 0$ , and  $\Omega(K) \rightarrow 1$ . Substituting Eq. (10) into Eqs. (8) and (9) yields a solution for  $K$  and  $\Omega$  which satisfies the above limits when the proper root is chosen, or

$$K = \frac{1 - \sqrt{1 - 2\cos^2 \sigma_J}}{\cos \sigma_J} \quad (11)$$

and

$$\Omega(K) = \left( \frac{2}{2 + K^2} \right)^{1/2} \quad (12)$$

The results of this type of analysis are shown in Table 1, where some tabulated values are listed for  $K$  and  $\Omega$  as a function of impingement angle for the assumed form of the azimuthal function  $f(K, \varphi)$ . Donaldson and Snedeker<sup>10</sup> measured the azimuthal variation of the velocity function and determined the azimuthal momentum flux per unit radian at a constant radial location. They represented these two quantities in the following nondimensional form which is here expressed in terms of the assumed velocity function

$$\tilde{V}_m(\varphi) = \frac{V_m(\varphi)}{V_m(\varphi=0)} = \frac{f(K, \varphi)}{f(K, \varphi=0)} \quad (13)$$

and

$$\tilde{M}_\varphi = \frac{\dot{M}_\varphi(\sigma_J, \varphi)}{\dot{M}_\varphi(\sigma_J = 90^\circ)} = \Omega^2(K) f^2(K, \varphi) \quad (14)$$

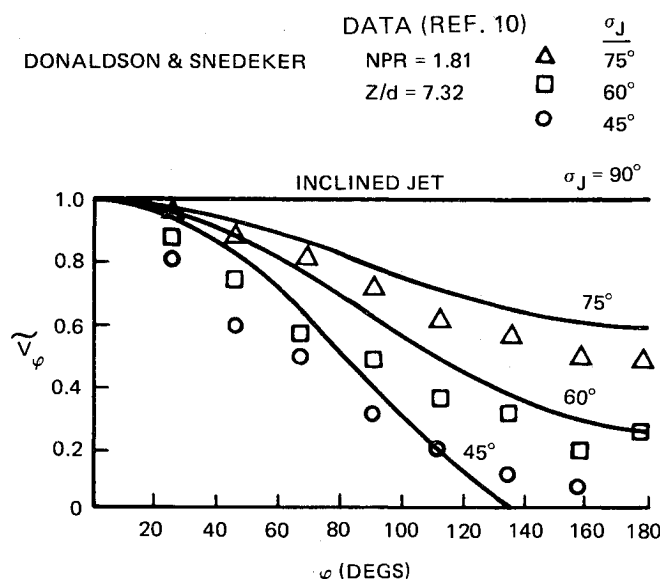
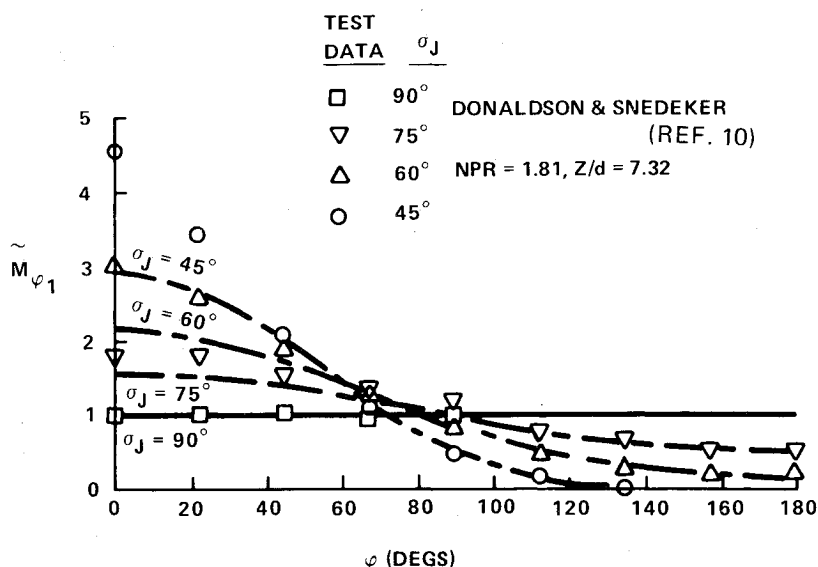


Fig. 3 Azimuthal wall jet velocity distribution.



A. COSINE FUNCTION

Fig. 4 Wall jet azimuthal momentum flux distribution.

Figures 3 and 4 show a comparison between Donaldson and Snedeker's data<sup>10</sup> for a nozzle pressure ratio of 1.81 and the results of the foregoing analysis. The cosine function behaves well at impingement angles close to 90 deg but does not yield physically acceptable results at impingement angles less than 52 deg.

Donaldson and Snedeker's data<sup>10</sup> indicate that, at some impingement angle just less than 45 deg, the upstream wall jet flow ( $\varphi = 180$  deg) is negligible. Figure 4 shows a comparison of the azimuthal momentum flux distributions for the assumed form of the azimuthal function and the distribution determined by Donaldson and Snedeker. Donaldson and Snedeker's data also showed a relative invariance of momentum flux distribution with nozzle total pressure ratio (NPR) for subsonic jets (NPR of 1.1-1.81).

### Generalized Stagnation Line Analysis

An analysis of the location of the stagnation line can now be derived without any further knowledge of the details of the wall jet flow situation and based purely on the foregoing momentum principles. In general, a vector momentum flux per unit area or "vector momentum density" can be defined as, for any wall jet  $j$ ,

$$I_{\varphi j} \equiv \left( \frac{1}{b_v} \frac{\partial \dot{M}}{r \partial \varphi} \right)_j i_{rj} = \rho C_s V_{mj}^2(r, \varphi) i_{rj} \quad (15)$$

Thus, it is seen that this "momentum density" is related directly to the maximum total pressure in the wall jet for a fully developed wall jet where the static pressure is ambient, or

$$I_{\varphi j} = 2C_s \Delta P_{mj} i_{rj} \quad (16)$$

This vector quantity can be further defined in terms of the azimuthal function as

$$I_{\varphi j} = \rho C_s \frac{(\beta \Omega)_j^2}{r^2} f_j^2(K, \varphi) i_{rj} \quad (17)$$

In terms of an arbitrary jet centered polar coordinate system (Fig. 5) defined by

$$\xi_j = \frac{X - X_{gj}}{e}, \quad \eta_j = \frac{Y - Y_{gj}}{e}, \quad r_j^2 = \xi_j^2 + \eta_j^2 \quad (18)$$

and

$$i_{rj} = \frac{\xi_j i_{xg}}{r_j^*} + \frac{\eta_j i_{yg}}{r_j^*}$$

where

$$e \equiv X_{g2} - X_{g1}$$

An expression for the location of the stagnation line can now be determined by imposing the condition, a priori, that the net "vector momentum density" normal to the stagnation line must be identically zero.

For two arbitrarily oriented oblique jets, this condition becomes

$$\sum_{j=1}^2 [I_{\varphi j} \cdot i_N] = 0$$

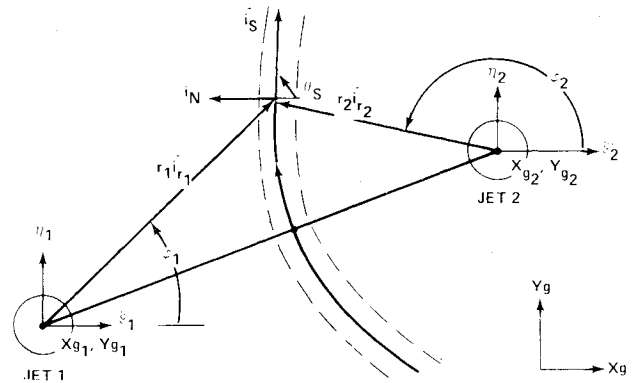


Fig. 5 Stagnation line analysis.

where

$$i_N = i_{yg} \cos \theta_s - i_{xg} \sin \theta_s \quad (19)$$

and  $\theta_s$  is defined to be the local inclination of the stagnation line. Equation (19) yields a first-order nonlinear ordinary differential equation for the ground stagnation line of the general form

$$\frac{dy_s}{dx_s} = \frac{\eta_1 r_1^* I_{\varphi 1} + \eta_2 r_2^* I_{\varphi 2}}{\xi_1 r_1^* I_{\varphi 1} + \xi_2 r_2^* I_{\varphi 2}} = \frac{I_{\varphi 2} \sin \varphi_2 - I_{\varphi 1} \sin \varphi_1}{I_{\varphi 2} \cos \varphi_2 - I_{\varphi 1} \cos \varphi_1} \quad (20)$$

where  $I_{\varphi j}$  is just the magnitude of the vector momentum density, Eq. (17). Equation (20) says that the ground stagnation line can be determined without regard to the actual profile shape or similarity constants of the wall jets, since this dependence drops out of the basic Eq. (19). This, of course, is only true if the stagnation line is established in a region where both wall jets exhibit similar profiles or are fully developed. Equation (19) does not apply if the stagnation line should be established within the impingement region of either jet.

In Ref. 4, the present momentum density balance analysis and a momentum flux balance method are each utilized to determine the location of the stagnation line. It is concluded that the present analysis is, in general, in better agreement with experimental data. Furthermore, the momentum balance technique<sup>5</sup> fixes the stagnation line position such that an upwash sheet normal to the ground is established. However, experimental upwash data, in the plane of symmetry of two jets, indicate that the upwash is indeed inclined relative to the ground in agreement with the current analysis. The "momentum density" approach further utilizes the momentum flux imbalance along the stagnation line to establish the flow inclinations in the upwash sheet, as will be described in the following section.

### Upwash Stagnation Point

Equation (19) can be used to determine an equation for the location of the upwash stagnation point that is situated on the line connecting the jet stagnation points. In fact, the integration of Eq. (20) proceeds from this initial point. Equation (19) reduces to

$$V_{m1}(r_{s1}, \varphi_1 = 0) = V_{m2}(r_{s2}, \varphi_2 = \pi) \quad (21)$$

or using Eq. (1),

$$\left( \frac{r_2}{r_1} \right)_s = \frac{(\beta \Omega)_2 f_2(K, \varphi_2 = \pi)}{(\beta \Omega)_1 f_1(K, \varphi_1 = 0)} \quad (22)$$



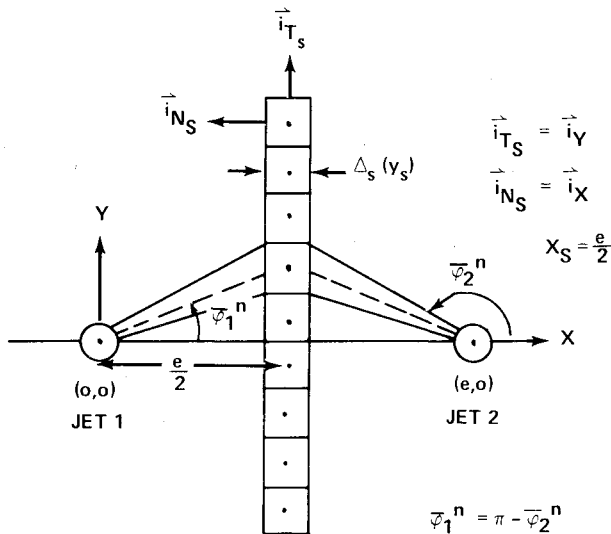


Fig. 8 Equal strength vertical impingement/upwash problem.

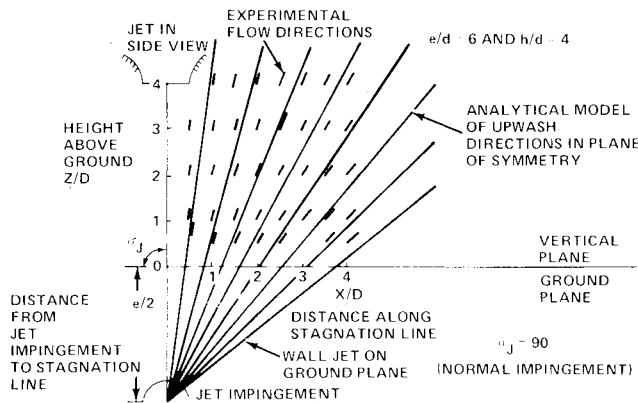


Fig. 9 Comparison of upwash flow direction model with experiment for two equal, vertical jets.

Since the jets are of equal strength, with impingement angle  $\pi/2$ , the stagnation line is trivially determined as  $x_s = e/2$ . In this case, any upwash element  $n$  is formed from equal wall jet azimuthal incremental angles  $|\delta\varphi|$ , i.e.,

$$|\delta\varphi_1^n| = |\delta\varphi_2^n|$$

and also

$$\bar{\varphi}_1^n = \pi - \bar{\varphi}_2^n$$

By substituting these identities into Eqs. (29) the following results are obtained

$$\begin{aligned} \cos\sigma_x^n &= 0 & \sigma_x^n &= \pi/2 \\ \cos\sigma_y^n &= \sin\bar{\varphi}_1^n & \text{or } \sigma_y^n &= (\pi/2) - \bar{\varphi}_1^n \\ \cos\sigma_z^n &= \cos\bar{\varphi}_1^n & \sigma_z^n &= \bar{\varphi}_1^n \end{aligned} \quad (30)$$

As expected, the upwash flow lies in the vertical  $y,z$  symmetry plane. The results also show that the upwash lateral inclinations appear as if the wall jet flow radial directionality was just reflected into the vertical plane. The analytical flow model is shown in Fig. 9 and is compared with measurements of the local flow inclination. The measurements were obtained by photographing an array of small paper flags that were located along the upwash centerline.

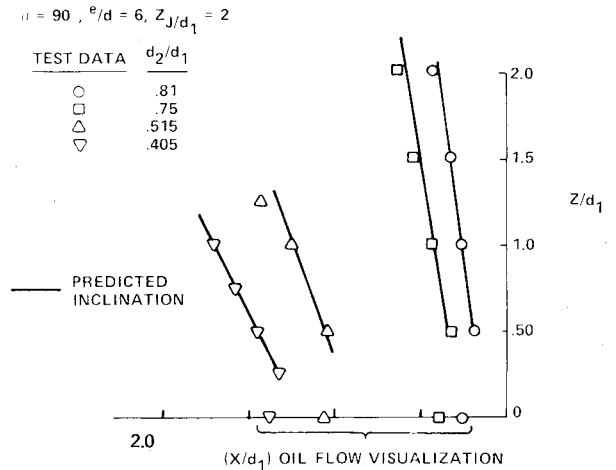


Fig. 10 Upwash inclination for unequal strength jets.

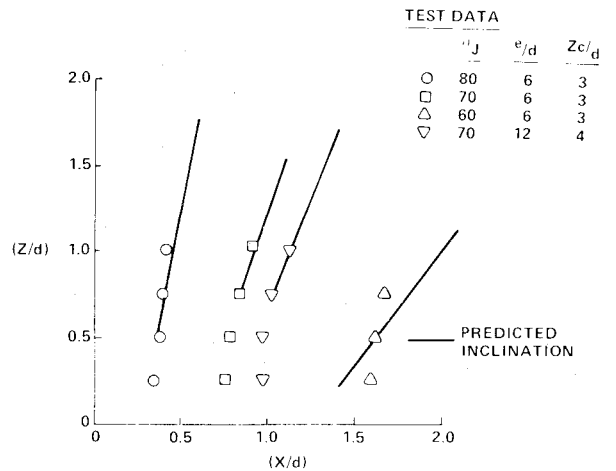


Fig. 11 Upwash inclination for equally inclined, equal strength jets.

### Comparison with Experiment

Several series of small scale experiments were conducted at Grumman's Research Jet Mixing Laboratory. Stagnation lines were determined by ground plane oil flow visualization techniques. Detailed pitot probe measurements and streamline visualizations were carried out in the upwash flow. Upwash trajectories in the vertical plane of symmetry were determined by tracking the location of the maximum total pressure with height above ground. All of the experiments were run using subsonic jets with uniform exit profiles at heights within the potential core of the jets. Several sets of experiments were conducted for unequal strength jets, achieved by unequal nozzle diameters, and equally inclined jets, achieved by rotating or inclining the ground plane. Most of the experiments were run with a nominal spacing of  $e/d = 6$  using a reference diameter jet of 2 in. Figures 10 and 11 show the trajectories of the upwash peak total pressure with height above ground for both unequal diameter vertical jets and equal strength inclined jets. Superimposed on these figures are the upwash angles predicted by Eq. (27) using Eqs. (23). For unequal momentum vertical jets, the upwash inclination was easily determined since the trajectories exhibited negligible curvature except in a region very close to the ground plane where the oil flow visualization measurements indicated a slight displacement. For equal strength inclined jets, the trajectories indicated more curvature to the upwash. For the two jets inclined at 60 deg, a large discrepancy between the predicted upwash angle and that indicated by measurements

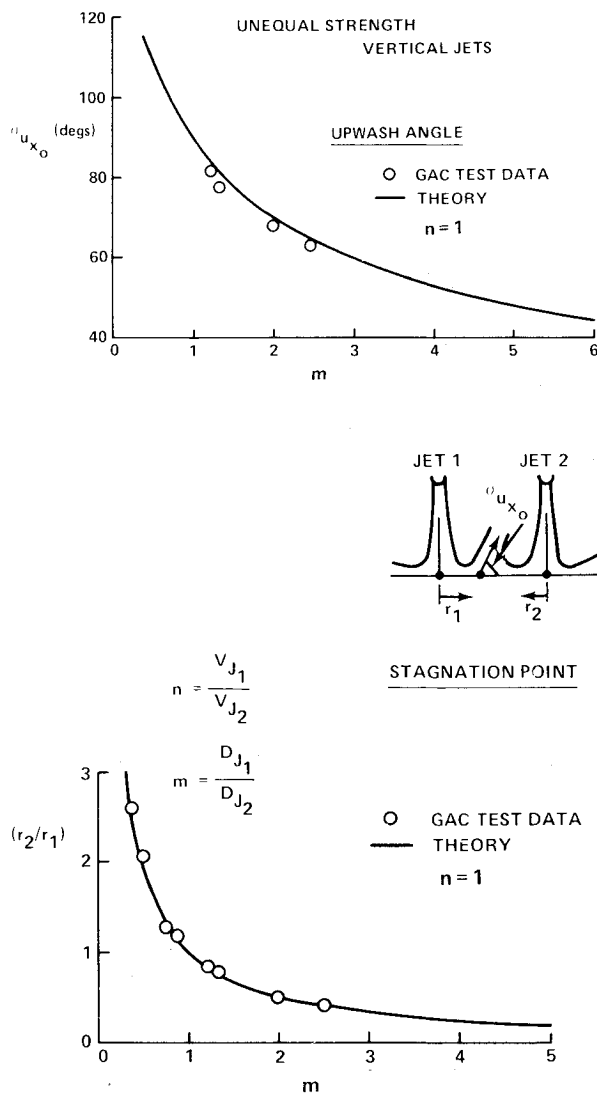


Fig. 12 Stagnation point and upwash inclination in the vertical plane of symmetry of unequal strength jets.

occurred. This may be due to the proximity of the upwash to the free jet impingement region and the occurrence of upwash recirculation.

Figure 12 shows a plot of the analytical results for unequal strength, vertical jets for stagnation point location and upwash angle in the plane of symmetry. Test data points are also shown. The stagnation point location was obtained from oil flow visualization techniques and the inclination angle from the upwash peak total pressure trajectory. Very good agreement was achieved using these simple analytical expressions.

Figure 13 shows a similar plot for equal strength inclined jets. The stagnation point location agrees well except at the smallest impingement angle. The experimental upwash inclination angles were obtained by determining the slope of the last two trajectory data points, shown in Fig. 11.

#### Stagnation Lines

Several parametric variations were run during the experimental phase of this study to determine the displacement and curvature of the stagnation line in the ground plane. Figure 14 shows the stagnation lines determined experimentally from oil flow visualization photographs. The results obtained by numerically integrating Eq. (20) are shown for comparison. The results are in fair agreement except at the smaller impingement angles.

The interesting aspect of these data is that the stagnation lines generated by jet inclination exhibit less lateral curvature than those for unequal momentum vertical jets. The largest discrepancy between data and numerical results occurs for the 60 deg impingement angle. For this angle, the stagnation line was shifted close to the rear jet and may be forming in the impingement region of this jet.

Additional experiments were conducted to show the effect of both inclination angle and diameter ratio on the stagnation line. Figure 15 shows the results of one experiment where both jets are inclined at 80 deg and the diameter ratio was unity and 0.687. The test was initially run with equal diameters. Then each jet was replaced, in turn, with a smaller nozzle. The stagnation line shifts accordingly. The numerical results for this problem are also shown and agree reasonably well with the test data.

#### STAGNATION POINT

TEST DATA

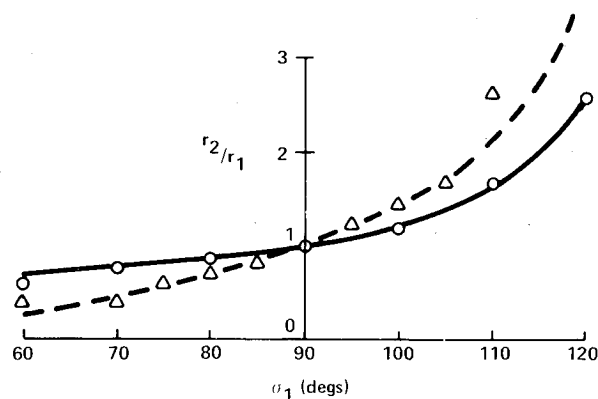
○ (REF. 2)  $\alpha_2 = 90^\circ$

△ GAC DATA,  $\alpha_1 = \alpha_2$

— THEORY ( $\alpha_2 = 90^\circ$ )

--- THEORY, ( $\alpha_1 = \alpha_2$ )

COSINE



#### UPWASH ANGLE

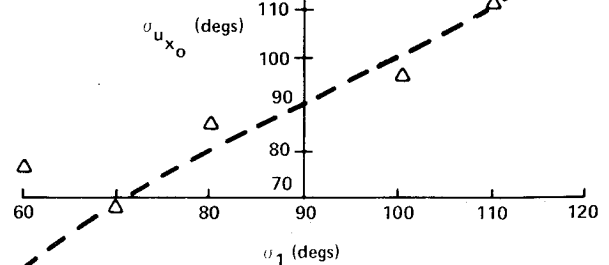


Fig. 13 Stagnation point and upwash inclination in the vertical plane of symmetry of equal strength, inclined jets.

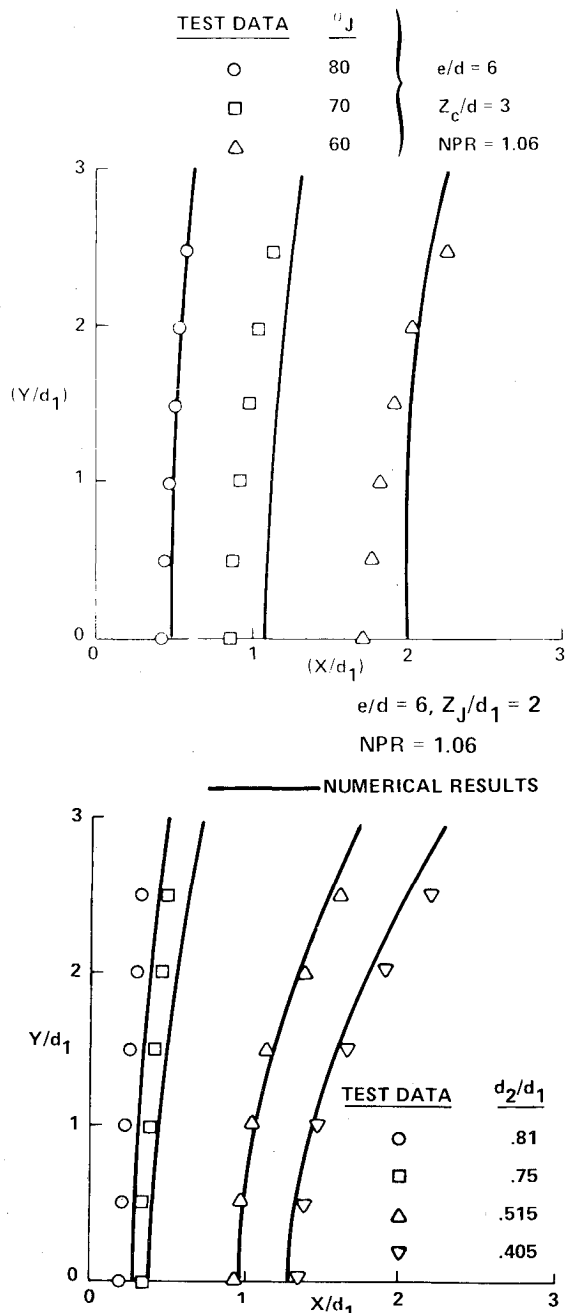


Fig. 14 Effect of jet diameter ratio and inclination angle on ground stagnation lines.

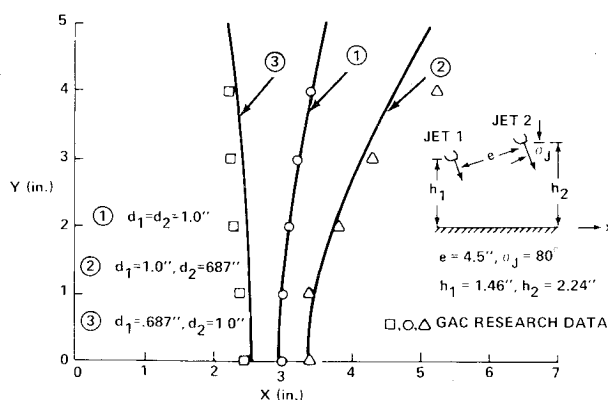


Fig. 15 Stagnation line behavior for equally inclined, unequal strength jets.

### Concluding Remarks

Simple analytical momentum models have been generated and shown to be reasonably successful in predicting several aspects of the wall jet interaction problem. The characteristics of the stagnation lines generated by unequal strength vertical jets are adequately predicted by the current models. Some discrepancies are apparent in the current model with respect to oblique jets at small impingement angles and further experimental as well as analytical investigation is recommended.

The "momentum density" approach allows for the determination of the stagnation line without performing a momentum flux balance differing from the approach of Refs. 4 and 5. The momentum flux imbalance established along the stagnation line then allows for determination of the inclination of the upwash sheet and individual flow vectors within the sheet. The upwash sheet in the present analysis is not necessarily normal to the ground plane.

### Acknowledgment

Portions of this study were sponsored under Navy Contract No. N0014074-C-0114, NAPTC, Trenton, N. J.

### References

- <sup>1</sup>Siclari, M. J., Migdal, D., and Palcza, J. L., "The Development of Theoretical Models for Jet-Induced Effects on V/STOL Aircraft," *Journal of Aircraft*, Vol. 13, Dec. 1976, p. 938.
- <sup>2</sup>Siclari, M. J., Barche, J., and Migdal, D., "V/STOL Aircraft Prediction Technique Development for Jet Induced Effects," Grumman Aerospace Corporation, Bethpage, N. Y., PDR 623-18, April 1975.
- <sup>3</sup>Siclari, M. J., Hill, W. G. Jr., and Jenkins, R. C., "Investigations of Stagnation Line and Upwash Formation," AIAA Paper 77-615, AIAA/NASA Ames V/STOL Conference, June 1977.
- <sup>4</sup>Kotansky, D. R. and Glaze, L. W., "Development of an Empirical Data Base and Analytical Modeling of Multiple Jet V/STOL Aircraft Flow Fields in Ground Effect," *Proceedings of the Workshop on V/STOL Aerodynamics*, Naval Postgraduate School, Monterey, Calif., May 16-18, 1979.
- <sup>5</sup>Kotansky, D. R., "The Influence of VTOL Vehicle Configuration Variables on Vectored Jet Induced Flow Fields in Ground Effect," AIAA Paper 78-1021, AIAA/SAE 14th Joint Propulsion Conference, Las Vegas, Nev., July 1978.
- <sup>6</sup>Kind, R. J. and Suthanthiran, K., "The Interaction of Two Opposing Plane Turbulent Wall Jets," AIAA Paper 72-211, AIAA 10th Aerospace Sciences Meeting, San Diego, Calif., 1972.
- <sup>7</sup>Siclari, M. J., Aidala, P., Wohllebe, F., Palcza, J. L., "Development of Prediction Techniques for Multi-Jet Thermal Ground Flow Field and Fountain Formation," AIAA Paper 77-616 AIAA/NASA Ames V/STOL Conference, Palo Alto, Calif., June 1977.
- <sup>8</sup>Adarkar, D. B. and Hall, G. R., "The 'Fountain Effect' and VTOL Exhaust Ingestion," *Journal of Aircraft*, Vol. 6, March-April 1969, p. 109.
- <sup>9</sup>Hrycak, P., Lee, D. T., Gauntner, J. W., and Livingwood, J. N. B., "Experimental Flow Characteristics of a Single Turbulent Jet Impinging on a Flat Plate," NASA TND-5690, March 1970.
- <sup>10</sup>Donaldson, C. D. and Snedeker, R. S., "Hypervelocity Kill Mechanisms Program," NRL Memorandum Report 1687, Aeronautical Research Associates of Princeton, Princeton, N. J., ARAP Report No. 64, April 1965.
- <sup>11</sup>Donaldson, C. D. and Snedeker, R. S., "A Study of Free Jet Impingement. Part I - Mean Properties of Free and Impinging Jets," *Journal of Fluid Mechanics*, Vol. 45, Pt. 2, 1971, pp. 281-319.